PHYSICAL REVIEW B VOLUME 36, NUMBER 15 15 NOVEMBER 1987-II

Process-induced and gold acceptor defects in silicon

A. Mesli, E. Courcelle, T. Zundel, and P. Siffert

Laboratoire de Physique et Applications des Semiconducteurs, Centre de Recherches Nucléaires, Boite Postale No. 20, F-67037 Strasbourg Cédex, France

(Received 19 September 1986; revised manuscript received 3 August 1987)

We report detailed measurements of the thermal properties of two different defects in silicon: the gold impurity and the process-induced defects generated by rapid thermal annealing. It is found that the ratio of the concentration of the gold acceptor to the gold donor is about 5, but both levels are completely hydrogen passivated, in contrast to other results reported in the literature. We have also measured the hole-capture cross section of the gold donor in *n*-type silicon and found a value of 1.8×10^{-14} cm^2 which is larger than that reported in *p*-type silicon. The second part of this work deals with the gold acceptor and the process-induced centers. We show that their electron thermal-emission rates are identical and field independent, at least up to 10^5 V/cm. Like the gold acceptor, the process-induced defect controls the thermally generated carriers in the depletion region. In contrast to the gold acceptor, we show that the total entropy of creation of *e-h* pairs, via the process-induced level, is very close to the entropy of the silicon band gap. The hole-capture cross section at the negatively charged gold-acceptor level decreases with the electric field which makes its temperature dependence weaker. However, the Coulombic potential does not properly fit the experimental results. Finally, it is reported that oxygen plays a crucial role in the stability of the process-induced defects generated by rapid thermal annealing. Our results support the hypothesis that the process-induced defect is probably the basis of the gold acceptor and perhaps other midgap levels, as already reported.

I. INTRODUCTION

Nonradiative generation-recombination centers induced by the transition-metal impurities in silicon are of fundamental importance from both a theoretical[1,2] and experimental viewpoint. They are characterized by the thermal-emission rate, the capture cross section, and the entropy factor accompanying the carrier release from deep levels.

The first parameter is a property of the ground-state energy and generally, for a given trap, it is accurately determined. However, in some circumstances, the theoretical predictions do not agree with the real behavior. For example, the electric field dependence of the hole thermal-emission rate from the gold-acceptor level, predicted by the three-dimensional Poole-Frenkel[3,4] theory, has not been experimentally verified[5–7] while for other defects it has been clearly identified.[8,9]

In contrast to the thermal-emission rate, the capture cross section and the entropy factor are strongly influenced by the shape of the defect wave function and possible excited states. Experimentally, many values have been quoted with large variations.[10] This is probably due to the interaction of the center with other impurities like the dopant and oxygen. Theoretically, it is very difficult to take these multiple interactions into account. Nevertheless, the temperature dependences for the attractive centers[11–13] as well as for the neutral centers[14–17] are well predicted. However, in the last case, some unexpected field effects have been observed.[18]

The gold impurity is among the best studied defects in silicon. These studies have accumulated a large amount of data involving many subtle controversial results although the effect of gold on the minority-carrier lifetime is universally admitted. Recently, Lang *et al.*[10] in their work on the complex nature of gold-related deep levels in silicon made a first attempt to reconcile the major results by a critical examination of the data available in the literature. From their work, the following two propositions emerged.

(1) The gold impurity is not a simple and well-defined defect but rather a family of different gold based complexes where the pairing with dopant and association with oxygen play a determining role.

(2) The process-induced defect constitutes the basic structure of a group of five chemical impurities (Au, Ag, Co, Rh, S), all characterized by midgap levels. Their thermal diffusion in silicon is controlled by a large complex of vacancies generated during the heat treatment, which also controls the transition from the mobile interstitial site to the final state. This final state would be characterized by thermal-emission properties fitted to the complex of vacancies and would be independent of the chemical impurities.

The first point stimulated many authors to find direct support for or against the proposal of Lang *et al.*[10] particularly concerning the pairing effect between the gold and the dopant[19] and the conflict as to whether the gold-donor and acceptor levels do[20–24] or do not belong[10,25,26] to the same defect. Unfortunately, the second proposal has never been confirmed and we believe that it can provide fundamental information for the understanding of diffusion and gettering of impurities in silicon.

In this paper we carry out complete analyses of the gold and process-induced defects. The complex of va-

 ©1987 The American Physical Society

cancies is created by rapid thermal annealing (here after called RTA) in the same basic material as used for gold diffusion. By using electrical and optical deep-level transient spectroscopy (DLTS), we analyze simultaneously the majority- and minority-carrier traps in Schottky diodes. The advantage in using this device is to avoid the complication arising when making junctions by implantation or diffusion.[27] However, as a consequence of the optical DLTS, the trapping and emission occurring in the high-field region cannot be separated in time. Consequently, numerical methods become necessary to extract the trap characteristics from the experimental data.

In Sec. II we detail the theoretical support and the numerical procedure for our experimental analysis. In Sec. III we describe the experimental conditions and techniques used in this work. The thermal capture and emission rates of carriers are discussed in Sec. IV. Then, we give our point of view on the relation between the gold donor and acceptor levels. The electric field dependence of the electron thermal-emission rates of the centers lying near the midgap are discussed in the same section. In the last part of Sec. IV, we present the recombination characteristics of such centers. Then, the electric field effect on minority-capture cross section is clearly shown and comparison with the theoretical predictions is made. In Sec. V we discuss the major points of this paper and the conclusions which may be drawn from the data related to the association of the gold-acceptor with process-induced defects. Finally, the correction procedure proposed to the method used by Sah *et al.*[28] to extract the electric field dependence of the emission rates is discussed in the Appendix.

II. THEORY

The capacitance transient measurements used in this work are based on the relaxation of trapped charges according to the kinetic equation.[29]

$$\frac{dn_T}{dt} = -n_T[e_n + e_p + c_n n(x) + c_p p(x)] + N_T[e_p + c_n n(x)] \ . \tag{1}$$

In the dark, $e_{n,p}$ and $c_{n,p}$ are the thermal-emission and capture rates, respectively. $n(x)$ and $p(x)$ represent the free carrier distributions. In the n-type Schottky diode, the transient capacitance signal is calculated by

$$\Delta C(t) = q\epsilon_r S \int_t \frac{1}{W_r^3(t)\rho(W_r,t)} \int_{\mathcal{D}} x \left[\frac{dn_T}{dt}\right] dx\, dt \ , \tag{2}$$

where ϵ_r is the dielectric constant, S the area of the device, and $W_r(t)$ the space-charge region where $\rho(W_r,t)$ is the fixed charge density. $\mathcal{D}$ is the spatial interval where the exchange of the trapped carriers occurs. This region must be known precisely in order to extract the true value of the concentration of the analyzed trap. It will depend on the initial conditions.

Equation (1), which is in general nonlinear, can be simplified to a linear form and then the parameters of the trap easily derived if both the capture and emission processes are temporally separable.[30] Unfortunately, in some cases this approximation does not hold and deviations from the linear form can occur, leading to large errors if the sources of these deviations are neglected. This may lead to controversial conclusions on some properties of the defects as will be discussed.

The first deviation arising in this work is the presence of free carrier tail in the depleted zone—an effect known as Debye incursion—due to the nonuniform density of the majority carriers available for capture.[31,32] Practically, this effect induces a competition of emission with capture at the crossing point W_0 in the space-charge region[33–37] (see Fig. 1). To overcome these difficulties, a large reverse bias and/or fitting method must be used in order to extract parameters such as the capture cross section.[36]

The second complication arises in the optical DLTS where competition of emission with capture occurs in the high-field regime and in the entire depleted region. Therefore, we cannot have a net temporal separation of these processes so that data treatment becomes more complicated.

A. Majority-carriers capture process

Taking the Debye effect into account, the exact rate equation is obtained from Eq. (1) when hole emission is neglected.

$$\frac{dn_T}{dt} = c_n(N_T - n_T)n(x) - n_T e_n \ . \tag{3}$$

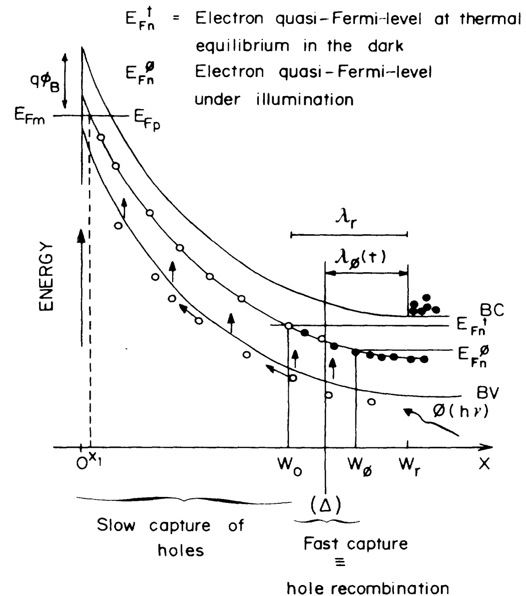

FIG. 1. Band diagram illustrating the capture of photogenerated holes in reverse biased n-type Schottky diode. $\lambda_\Phi(t)$ is the transition region during the relaxation (after the light is switched off). It corresponds to λ_r at thermal equilibrium.

According to the distribution $n(x)$, two parts of the space-charge layer must be considered. The neutral portion where $n(x)$ is uniform $[(n(x)=N_D]$ and the region where $n(x)$ is very small. Thus at some point $c_n n(x)<e_n$, and emission becomes significant. Resolving Eq. (3) and integrating Eq. (2) yields the majority transient capacitance relation:

$$\Delta C(t)=\frac{C_r^3}{(\epsilon_r S)^2}\frac{N_T}{N_D}\exp\left[\frac{-t}{\tau_e}\right]\times\int_{W_F-\lambda_r}^{W_r-\lambda_r}\frac{1-\exp\left[-\frac{t_F}{\tau_{\rm co}}\left[\frac{n(x)}{N_D}+\eta\right]\right]}{1+\eta\frac{N_D}{n(x)}}x\,dx\ , \tag{4}$$

where C_r is the capacitance at reverse bias V_r, λ_r the transition region as indicated in Fig. 1, $\tau_{\rm CO}$ $(=1/c_n N_D)$ and τ_e $(=1/e_n)$ are the capture and emission time constants, respectively, under zero electric field. $\eta=\tau_{\rm CO}/\tau_e$, t_F the DLTS pulse duration, and $n(x)$ obeys the relation

$$n(x)=N_D\exp\left[-\frac{(W_F-x)^2}{2L_D^2}\right]\ , \tag{5}$$

where W_F is the depleted zone under forward bias and L_D is the Debye length.[36] In (4) we suppose the emission rate to be field independent as was the case in our experiments. If a staircase approximation is used (negligible Debye tail effect), from (4) we find the expression (3.13) of Ref. 37 with $\eta\mapsto 0$ and $n(x)=N_D$.

B. Minority-carriers capture process

In the Schottky diodes used in this work, the minority carriers are generated by subband gap light excitation absorbed through the semitransparent contact. This technique, recently introduced,[38] is known as minority-carrier transient spectroscopy (MCTS).

If the level is located in the lower half of the gap, the thermal ionization rate for the majority carriers (electrons) is very small because of the large energy E_c-E_T in the Boltzmann factor of the detailed balance expression for e_n. Thus the hole thermal emission dominates and the Debye tail effect becomes ineffective. However, in contrast to the classical DLTS procedure, the minority carriers are trapped in the depleted zone where the emission probability cannot be neglected during the illumination process. Thus, Eq. (1) is reduced to

$$\frac{dp_T}{dt}=-\frac{dn_T}{dt}=c_P(N_T-P_T)p(x)-P_T e_p\ . \tag{6}$$

Neglecting the photoionization process,[38] e_p still remains the thermal-emission rate. As compared to Eq. (3), the kinetics of trapping in MCTS is controlled by the nonuniform hole distribution available for capture. $p(x)$ represents the photogenerated minority-carrier density flowing in the depleted zone given by

$$p(x)=\frac{J_{\rm ph}(1-x/W_r)}{q\mu_p\langle\mathcal{E}_m\rangle}\ , \tag{7}$$

$\langle\mathcal{E}_m\rangle$ is the maximum electric field at the surface. $J_{\rm ph}$ is the photocurrent and μ_p is the hole mobility. Depending on the strength of the electric field, μ_p is field independent[39] or not.[40] With $p_T(x,t)=0$ at $t=0$, the minority transient capacitance is derived from Eqs. (6) and (2). It follows that

$$\Delta C(t)=\frac{N_T}{N_D}\frac{C_r^3}{(\epsilon_r S)^2}\exp(-e_p t)\times\int_{\mathcal{D}}\frac{c_p p(x)}{c_p p(x)+e_p}\{1-\exp-[c_p p(x)+e_p]t_F\}x\,dx\ , \tag{8}$$

where e_p is assumed to be field independent. The spatial region $\mathcal{D}$ is deduced from the examination of the behavior of the quasi-Fermi-levels under reverse bias conditions in the dark[41] and under illumination.[42,43] According to Fig. 1, the lower limit x_1 of $\mathcal{D}$ corresponds to the dark condition and is determined by $E_T(x_1)=E_{Fp}$ where we take the Fermi level in the metal as the zero energy.[41] Under illumination, we show that the splitting of the equilibrium Fermi level occurs deeply in the neutral region[42,43] such that the upper limit of the domain $\mathcal{D}$ is equal to W_r.

In the particular situation where the levels is close to the midgap, the Debye tail incursion becomes effective and then the capacitance response becomes more complicated. As shown in Fig. 1, the effective region involves two parts separated by the front Δ: $0<x<W_0$ where $E_F>E_T$ and the transition region $W_0<x<W_r$ where $E_F<E_T$. This front moves during the relaxation giving rise to a fast transient followed by a slow one. Figure 2 shows the semilog plot of the total transient recorded for the neutral gold acceptor in n-type silicon.

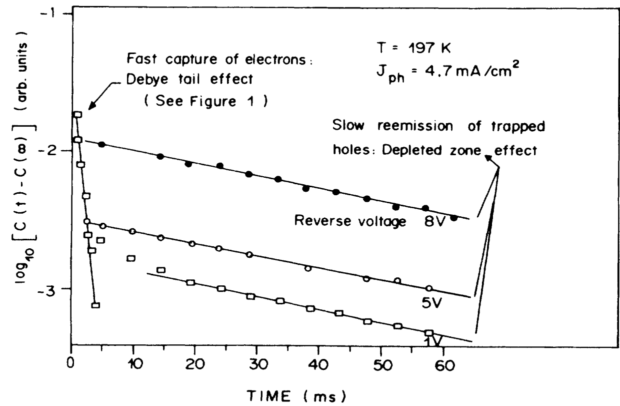

FIG. 2. Capacitance transient after optical excitation. The long-time constant corresponds to the emission of holes from the gold-acceptor level. The shortest time constant represents the Debye tail effect occurring in the transition region $\lambda_r-\lambda_\Phi(t)$.

It appears that the fast component vanishes or becomes negligible at high reverse bias. In this work we use the method proposed by Vincent[44] to remove the "transition region perturbation." It involves a slight decrease in the reverse bias (some mV) during the illumination. Two cases have to be considered.

If the diode is kept at reverse bias, the transient capacitance, due to the minority-carrier (holes) emission, is expressed by the relation (8) where $\mathcal{D}$ extends from the surface to $x = W_0$.

If the device is forward biased before optical excitation, we take up the double pulse method as described by Lang.[45] The procedure consists of placing all the traps below the electron quasi-Fermi level by forward biasing the device before the optical pulse of duration t_F. Thus according to Eq. (1) where only e_n and $c_p p(x)$ are significant for $0 < t < t_F$ and where e_n is dominant at $t > t_F$, the density of the nonrecombined part of the injected electron is given by

$$n_T(x,t) = N_T \exp[-c_p p(x) t_F] \exp(-e_n t) \ . \tag{9}$$

Using this relation and integrating (2), we obtain the so-called DLTS-clear transient with the same spatial domain as above.

C. The numerical method

Under the complications mentioned above numerical methods become necessary in order to extract the trap parameters. In this work we have used the least-square fitting technique which is reasonably valid for a single exponential and a large signal-to-noise ratio.[46] It consists, in the first step, of digitizing the whole transient capacitance at a given temperature. Then, we search for m parameters P_j $(j=1,2,..,m) = e_n, e_p, N_T$ so that Eqs. (4) and (8) represented by $Y_f(t_i, P_j)$ will be a least-square fit of the data points $Y_i(t_i)$ where t_i are the sampling time points:

$$\min_{P_j} \left[\sum_{i=1}^{n} [Y_i(t_i) - Y_f(t_i, P_j)]^2 \right] , \tag{10}$$

where "min" represents the minimization of the sum mentioned above. For multiple exponential transients there are more accurate methods based on the deconvolution principle.[47] The thermal-emission rates extracted from relation (10) at fixed temperature are injected in expressions (4) and (8). The effective fraction of empty traps at the end of the filling pulse given by $1 - S(t_F)/S(t_F \to \infty)$ is independent of the trap concentration. For a pulse duration t_F, $S(t_F)$ is the DLTS or MCTS signal obtained from relations (4) and (8), respectively. Thus

$$S(t_F) = \Delta C(t_1) - \Delta C(t_2) \ , \tag{11}$$

where t_2/t_1 $(=2.5)$ is kept constant. Since t_F and τ_e are known at every data point, the fit is performed by adjusting only the capture parameter.[36] In particular, for the majority-capture cross section measurements, τ_{CO} is adjusted for the best fit to the short t_F data where a linear behavior is observed. Then we use the resulting capture time constant τ_{CO} to estimate η $(= \tau_{CO}/\tau_e)$ and repeat the calculation using η to get a better estimate of τ_{CO}. Finally, for a given t_F, we record the DLTS and MCTS peak heights as a function of the temperature peak maxima corresponding to different rate windows. The best fit is obtained by adjusting N_T.

III. EXPERIMENTAL CONDITIONS

The silicon samples used in this study were taken from P-doped floating zone and Czochralski grown crystals. The phosphorus density is $(1-5) \times 10^{15}$ cm^{-3} and the stray impurities densities are lower than 10^{11} cm^{-3}. Various wafers were gold diffused at 900 °C to give the bulk homogeneous concentration around $(3-4) \times 10^{14}$ cm^{-3}. Samples from the same material were separately treated in a rapid heat pulse system. As we will see later in the experimental results, it was necessary to study the role of the surface preparation prior to thermal (RTA) treatment. For this purpose some samples were atomically damaged (lapped) in a depth of 200 Å from the surface while others have been chemically etched in order to minimize the surface defects. The thermal cycles, performed in argon atmosphere, are computerized and the heat pulse rise time fixed at 1 s. The duration of the heat plateau at a given temperature varied from 5 to 40 s. The cooling rate was taken at 300 °C/s. The samples were quenched from temperatures of 800 to 1200 °C.

All the samples were used for Schottky diode preparations. Semitransparent Schottky contacts were evaporated at the top of the silicon substrates Au-Φ (120–150 Å) through a window in the predeposited oxide thin film. The back contacts (Ohmic) were aluminum evaporated. The experimental techniques used in this work consisted of Schottky space-charge spectroscopy. A modified boonton capacitance meter is used with a fast pulse interface for capture cross-section measurements (pulse duration ranging from 10 nsec to unlimited upper values). The sample temperature is measured by a Pt(100) resistance thermometer located in the sample holder. The thermal stability is better than 0.1 K. For MCTS measurements, the optical source contains a GaAs double heterostructure diode. The wavelength at the peak intensity is 850 nm. The DLTS clear procedure used in this work is very similar to the one developed by Lang.[45] For the data treatment, we use a boxcar averager (EGBG 4420/99 model) connected to a computer (Hewlett-Packard-9816A) suitable for speed calculation and data treatment. For each temperature interval, from 1 to 4096 data points are taken from the capacitance transient. Then, they are averaged for noise reduction, stored in an internal buffer, and transferred to the host computer for transient measurements. The gate widths vary from 2 ns to 2 ms depending on the noise level.

IV. EXPERIMENTAL RESULTS

Figures 3 and 4 show DLTS and MCTS spectra for the gold-doped Schottky diodes and the process-induced defects generated by RTA, respectively. The control sample (without gold) treated by the same thermal cycle

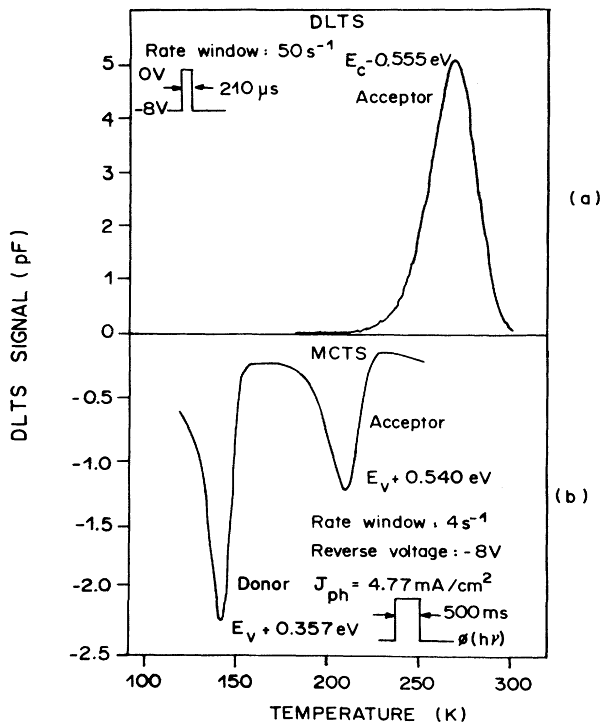

FIG. 3. Transient thermal spectroscopy of the gold-doped *n*-type Schottky diode. Positive signal corresponds to electron emission (DLTS) while negative peaks correspond to hole emission (MCTS).

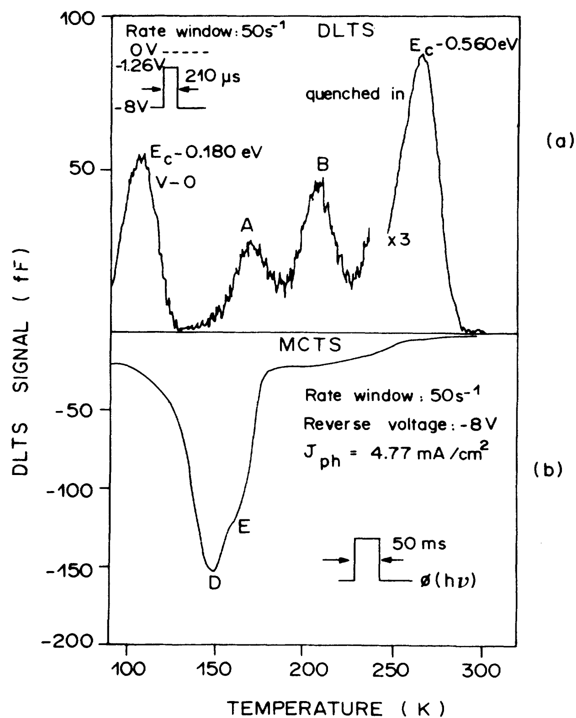

FIG. 4. Similar spectra as in Fig. 3 recording the process-induced levels after 1000 °C treatment in the heat pulse during 5 s followed by a quenching to 25 °C at 300 °C/s. No difference is observable after 35 μm removal, showing a uniform distribution of the defects deeply in the material.

as the gold diffused ones were checked for transient response and none was observed over the temperature range of DLTS scan at sensitivities up to the residual impurities content (10^{11} cm^{-3}). In Fig. 3 we observe the classical DLTS spectrum of the gold-acceptor (positive peak) and the gold-donor (negative peak at 150 K) levels. The deeper minority trap (peak at 220 K), not present in the control sample, does not anneal out at 650 °C during 1 h. Thus it cannot be assigned to any structural defects generated mainly by thermal stress at high cooling rates as we will see below. Thus we conclude that the level $E_V + 0.54$ eV is due to the relaxation of hole occupancy taking place at the gold-acceptor level as previously seen in *p*-type material.[23,48] It interacts with the conduction and the valence band as we should expect from a neutral recombination center for which the sum of thermal activation energies for both carriers is closer to the silicon gap ($\simeq 1.095$ eV).

Figure 4 shows that the RTA process introduces a large number of levels but with small concentrations, especially for the peaks labeled *A*, *B*, *D*, and *E*. These levels have a somewhat complicated origin as recently observed in classical thermal quenching experiments.[49] Nevertheless, intrinsic impurities in the basic material with large densities such as oxygen seem to play an important role in the formation of these defects.[50] The $E_c - 0.18$ eV level is very likely the *V*-O center often reported in high-oxygen content *CZ* materials ([O] > 10^{17} cm^{-3}) which have undergone treatments involving the creation of vacancies above the equilibrium concentration. Actually, for the same RTA treatment, the density of this defect is strongly dependent on the surface preparation. As shown in Fig. 5, the peak height of the level $E_c - 0.18$ eV is reduced by a factor of 2 when the material is chemically etched (i.e., low density of vacancies at the surface) instead of being atomically damaged

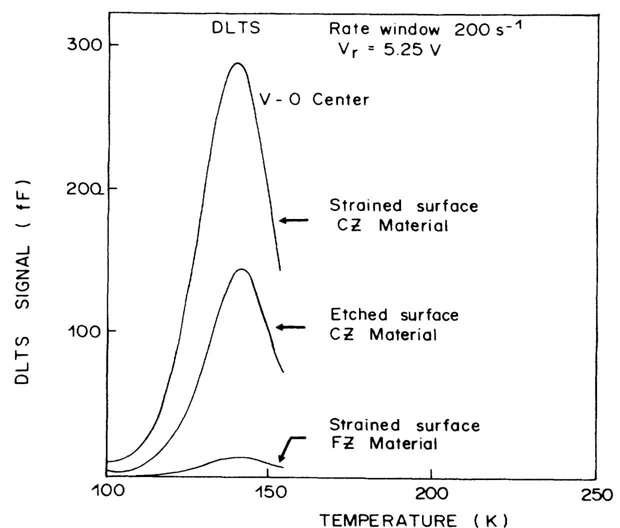

FIG. 5. The *V*-O (*A* center) peak height as a function of the oxygen content and the surface preparation prior to three successive cycles of RTA treatment (1000 °C for 40 s) followed by a quenching to 25 °C at 300 °C/s.

(strained surface) prior to RTA treatment. In the same figure, we show that even for a lower oxygen-content (*FZ* material), the high concentration of vacancies at the surface may increase the probability of formation of the *V*-O center. Since this paper deals mainly with the study of the levels located in the midgap of silicon, we will focus our attention only on the level $E_c-0.56$ eV—called the process-induced defect—which presents the highest concentration. This defect generated at high temperature and quenched in by fast cooling, cannot be assigned to gold contamination even though it has the same energy level as the gold acceptor. Moreover, its total annealing is reached in a classical furnace at 650 °C (1 h). As shown in Fig. 4(b), for such class of midgap levels, a MCTS peak should appear interacting with the valence band if the equilibrium charge state is 0 or negative. This is not the case even for large minority-carrier injections. Thus the level $E_c-0.56$ eV is of a donor type as stated before by Yau *et al.*[51] for the same defect.

Finally, we must point out that a careful DLTS analysis is necessary to avoid erroneous interpretations. Actually, as mentioned in Fig. 4(a), the filling pulse voltage applied in DLTS does not exceed -1.26 V. This limitation is due to an unusual effect occurring especially in Schottky diodes. This phenomenon has been analyzed in detail more recently,[52] where the concept of pseudo-Fermi levels of holes and electrons explains very well this behavior.[41,52,53] The major problem arising from this subtle anomaly is the possible screening of a majority level (in our case the *V*-O peak) by a minority trap, complicating the interpretation of the experimental data.

A. Thermal capture cross sections and emission rates for gold and process-induced levels

1. Capture cross sections

The capture data points for gold levels are shown in Fig. 6. The ordinate is the effective fraction of empty traps at the end of the filling pulse. For the electron capture (majority carrier) at the gold acceptor, $S(\infty)$ is taken at $t_F=2$ μs (doping 5×10^{15} cm^{-3}) for which saturation of the trap is reached. However, for the hole capture (minority carrier) at the gold donor, $S(\infty)$ is considered at $t_F=200$ ms because of the very low density of the photogenerated minority carriers. The data of Fig. 6 indicate clearly that the Debye tail effect, more effective for long filling pulses in DLTS measurements (solid circles), is less critical than the nonzero field phenomena taking place in MCTS (open circles) where we observe a total deviation from the linear behavior. It makes intuitive sense that the Debye tail incursion involves only a fraction of the depleted zone while the nonzero field regime affects the whole space-charge layer. Thus the capture cross sections are determined numerically as indicated in Sec. II. The fitting plots are represented by the solid lines in Fig. 6, and the extracted values are listed in Table I.

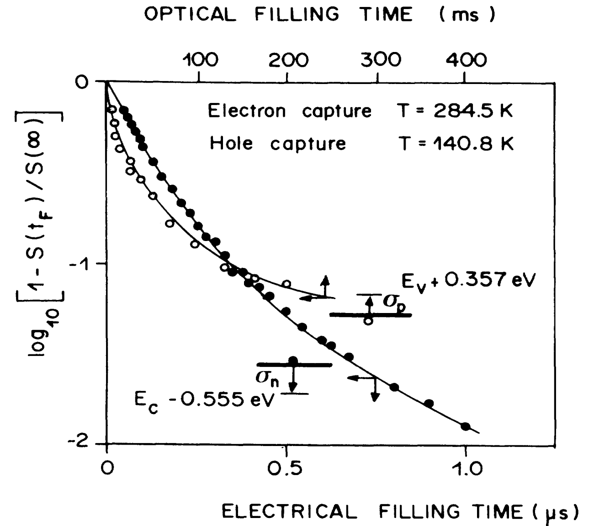

FIG. 6. DLTS and MCTS trap filling data for the gold-acceptor and donor levels, respectively. The effective fraction of empty trap at the end of the filling pulse is plotted vs filling pulse width. The solid lines represent the fitting plots.

The electron-capture cross section of the gold acceptor falls in the range of the first group ($N_{Au} \ll N_D$) of Lang's classification[10] and is temperature independent.

TABLE I. Thermodynamic parameters of the gold-acceptor, donor, and process-induced levels.

Defect	Charge state	Enthalpy reaction $\Delta H_{n,p}$ (eV)	Capture cross section $\sigma_{n,p}$ (cm^2)	Temperature dependence of $\sigma_{n,p}$	Electric field measurement (V/cm)	Entropy factor $\Delta S_{n,p}$	Literature
Au acceptor (e^- trap)	(0,−)	0.555	9×10^{-17}	200–300 K	0	3.9 K $X_n=51$	See Tables I and II in Ref. 10 and Table I in Ref. 56
Au donor	(0,+)	0.356	1.8×10^{-14}	100–180 K	5.10^4 no field dependence	3.2 K $X_p=26$	See Table 3 in Ref. 56 and Table I in Ref. 57
Process-induced defect (donor)	(+,0)	0.560	(2×10^{-15} at 300 K)	T^{-1} 200–300 K	0	1.5 K $X_n=4.6$	Yau *et al.* (1974) $\sigma_n \propto T^{-0.73}$ at 1.6×10^4 V/cm $\sigma_n=1.42\times10^{-13}$ cm^2 at 300 K

This group has the smallest capture cross section values as compared to the others: i.e., $N_{Au} \simeq N_D$ and $N_{Au} \gg N_D$. This classification suggests that some ion-pairing phenomenon between the gold impurity and the shallow dopant (most likely P) might be taking place when $N_{Au}/N_D > 1$. However, this question remains open at the present time,[19,54,55] mainly because measurements in the range of the non-negligible N_T/N_D become a very delicate task. As far as the gold donor is concerned, very few authors have measured the hole-capture cross section directly in n-type silicon. A five times difference is found between our value and those quoted by Wu *et al.*[56] who made similar measurements (MCTS) on similar samples (n-type Czochralski doping, 10^{15} cm^{-3}). However, our results do agree with the value of 10^{-14} cm^2 estimated by Lang *et al.*[10] in p^+-n epitaxial junction, except that our measurements have been made under a high electric field, but no dependence on this parameter has been observed. We must point out that the value around 10^{-14} cm^2 is somewhat large as expected for a neutral center. The comparison with the values reported in the literature[56,57] shows clearly that our value is nearly an order of magnitude larger than in p-type silicon. This observation supports the idea that a complex formation of gold atoms with donors or acceptors affecting the physical nature of the defect cannot be fully excluded.[10]

The situation is less confusing for the electron-capture cross section at the process-induced level. From our measurements a value of 2×10^{-15} cm^{-2} is found at 300 K with T^{-1} variation as consistent for a donorlike defect $(+,0)$. However, this temperature dependence remains weaker than the predicted T^{-n} ($n=2$–5) function established for the Coulombic center.[12,13] The only direct measurement of the capture cross section available in the literature is due to Yau *et al.*[51] who found a $T^{-0.73}$ dependence at $\mathcal{E}=1.6\ 10^4$ V/cm. The extrapolation at 300 K gives a value of 10^{-13} cm^2 which is unusually higher.

2. Thermal-emission rates

According to the thermodynamic concept,[10,58] the thermal-emission rates are expressed in terms of the enthalpy reaction $\Delta H_{n,p}$ related to the exchange of carriers between band states in the gap and the conduction or valence band, and the entropy factor $\Delta S_{n,p}$ accompanying the electron (hole) emission. The last parameter takes into account the spin degeneracy and lattice relaxation contribution.[10] It is given by

$$e_{n,p} = X_{n,p}\sigma_{n,p} V_{n,p} N_{n,p} \exp(-\Delta H_{n,p}/kT)\ , \qquad (12)$$

where

$$X_{n,p} = \exp(\Delta S_{n,p}/k)\ .$$

N_n and N_p represent the state density of the conduction and valence bands, respectively.[59] By taking into account the standard correction of T^2, the Arrhenius plot of expression (12) is shown in Fig. 7. The extracted values $\Delta H_{n,p}$ and $\Delta S_{n,p}$ are reported in Table I. In the case of the process-induced level ΔH_n is corrected to the T^{-1} dependence of σ_n.

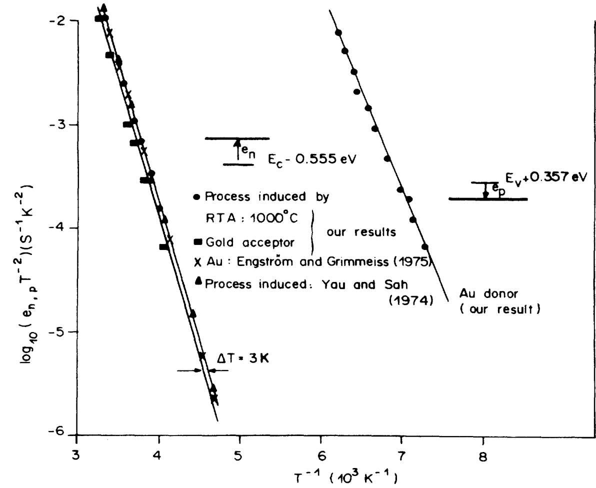

FIG. 7. Electron and hole thermal-emission rates vs reciprocal temperature for the gold and process-induced defects compared to those reported in the literature.

The entropy factor is one of the most controversial parameters of deep levels in silicon. In particular, for the gold acceptor attempts to reconcile the total entropy of the creation of an e-h pair via this level with the entropy of the silicon band gap have been difficult to realize.[10] $\Delta S_{n,p}$ is often obtained from the extrapolation of the thermal-emission data and its value depends strongly on the accuracy of measurements of $\Delta H_{n,p}$ and $\sigma_{n,p}$. As shown in Table I, the entropy factors are closer to those of Lang *et al.*[10] for the gold acceptor and those of Kassing *et al.*[57] for the gold donor while in the latter case the material has been p-type. For the process-induced defect the entropy factor is low showing a weak contribution of lattice relaxation to the creation of the e-h pair via this level.

However, concerning the thermal-emission rate which is a property of the ground state, a close similarity between the gold acceptor and the process-induced defect is shown in Fig. 7, while they are distinguishingly different defects. The slight difference in the extrapolated value $X_{n,p}\sigma_{n,p}$ between our results and those of Engstrom *et al.*[60] for the gold acceptor can be related to the oxygen content because of the different materials used in Ref. 60 (epitaxial n-type silicon) and in our analysis (Czochralski-grown n-type silicon). This behavior has been considered by Lang *et al.*[10] to support the fact that the gold defect formation sets oxygen in action and thus cannot be seen as a simple substitutional atom. Note that the thermal-emission rates of our process-induced defect and those of Yau *et al.*[51] are very close while N_T/N_D are completely different (0.6 in Yau's results and 10^{-3} in the our's) but both results are obtained from Czochralski-grown n-type silicon.

In consequence, as long as we do not obtain more information on the exact influence of oxygen and shallow dopant on the formation of the gold complex, we cannot conclude that the gold defect is a simple and unique defect. However, regarding the ground state which is

characterized by the thermal-emission rate, a surprising similarity is observed between the gold acceptor and the process-induced defects.

B. On the concentration of the gold-donor and acceptor levels

Figure 3 might suggest that the gold donor and acceptor levels do not belong to the same defect. However, for the reasons mentioned in Sec. II, more care should be taken in extracting concentrations. This must be done by taking into account all the parameters and their temperature dependence as expressed in (4) and (8). Figure 8 shows the DLTS and MCTS peak height variation with the temperature T_m. By numerical treatment, we find a value of 5 for the ratio N_T(acceptor)/N_T(donor) which should imply that these two levels do not belong to the same defect as stated by Lang *et al.*[10]

Based on the same kind of measurements, other authors[23,24,56] find that the two levels have the same concentration. In order to reach this result, Van Staa *et al.*[23] assumed that the hole-capture cross section of the negatively charged gold acceptor is temperature independent. This assumption contrasts with the well-established temperature behavior of this parameter. Recently, Ledebo *et al.*[21] performed other measurements in *p*-type silicon and concluded for a multiple charge state system. Pearton *et al.*[25] found that the gold donor and acceptor levels do not passivate in the same way. However, they did experiments on *n*- and *p*-type silicon in order to study the acceptor and donor levels as majority processes. Thus as long as it is not proved that the gold impurity behaves identically in *n*- and *p*-type material, we believe that it is more rigorous to study this impurity in the same basic material. To investigate this point experimentally, hydrogen passivation procedures were made using 2 keV, 10^{16} H^+/cm^{-2} implantations at 300 °C. The sample was etched (1000 Å removal) in order to remove the excess hydrogen near the surface and the damaged region. The DLTS and MCTS spectra were flat at sensitivities up to 10^{11} cm^{-3}. We conclude that this kind of experiment cannot put an end to the controversy arising from the relation between the gold donor and acceptor levels.

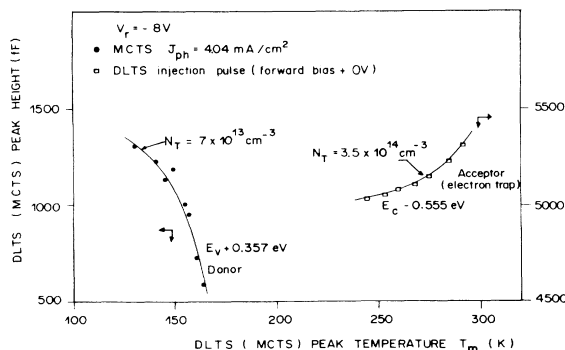

FIG. 8. Temperature dependence of the DLTS and MCTS peak heights of the gold acceptor and donor, respectively. T_m is recorded for different rate windows. Solid lines are calculated according to relations (4), (8), and (11) by adjusting the concentration N_T.

C. Field dependence of the thermal-emission rates

Among the fundamental physical properties of the gold acceptor and process-induced levels as generation-recombination centers, are the field dependence of their thermal-emission rate. The validity of the well-known detailed balance equation established at thermal equilibrium is usually determined from this dependence. This fact has been used by Lang *et al.*[10] to discuss the discrepancy between theory and experiment on the entropy of the *e*-*h* pair creation via the gold acceptor.

Based on the differential capacitance-decay curve measured between two nearly equal bias voltages,[28] the electric field dependence of e_n has been investigated by Tasch and Sah[5] in Au-doped Si and by Yau and Sah[51] for the process-induced defects in Si. In the two cases, a pronounced field dependence of the thermal-emission rate has been observed. In this work we investigate the electric field dependence according to the procedure described in Sec. II. The observation of a possible nonexponentiality according to expression (4), where τ_e must be spatially dependent, should be facilitated by working at low temperatures on substrates with large concentrations of dopant. In Fig. 9 we report measurements as well as the literature data. A large disagreement appears which is only apparent. As shown in the inset the tran-

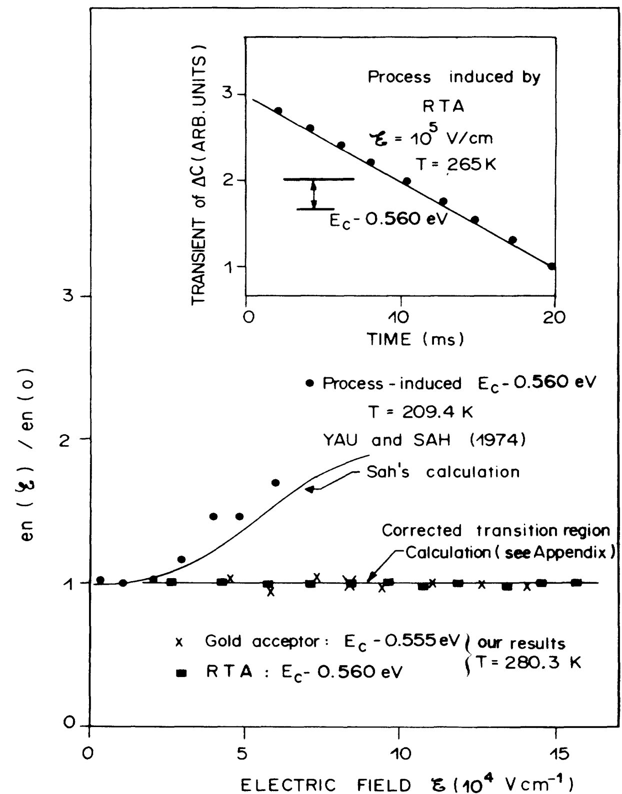

FIG. 9. Field dependence of the electron thermal-emission rates of the gold-acceptor and process-induced levels as compared to the result of Yau and Sah (Ref. 51). Solid lines correspond to the calculations developed in the Appendix. $e_n(0)$ is considered at 10^4 V/cm. In the inset we show the field-independent thermal-emission rate of the process-induced level.

sient is a pure exponential under any field in the range $\leq 10^5$ V/cm. In fact, the method used by the above-mentioned authors is based on the resolution of Poisson's equation, where they assume a negligible effect of the transition region. In the Appendix we show that this hypothesis is no longer valid, especially when the height of the pulse decreases.

Applying the Sah's[28] calculations to our experimental data, a field dependence appears closer to the results of Tasch, Yau, and Sah as shown in Fig. 9. Thus from our calculation we conclude that there is obviously no discrepancy between our experimental data and those of the literature. Consequently, within the experimental error, no field dependence of e_n is observable for average fields below 10^5 V/cm either for the gold acceptor or process-induced levels.

For the first level, Lax's model[11] predicts that the electron is bound to a short-range neutral polarization potential well of the form

$$V(r) = -A/r^4 ,$$

where $A = q^2 a^2/(4\pi\epsilon_r)^2$ and a is the polarizability of the neutral atom. Lax estimated A to be 2×10^{-31} eV cm^4. For $A \leq 2\times10^{-31}$ eV cm^4, there is a good agreement between theory and our data. Thus the value of A ($\simeq 2\times10^{-29}$ eV cm^4) quoted by Tasch and Sah,[5] which fit their experimental data seems to be very high (100 times the Lax's value) and probably related to the procedure used to measure $e_n(\mathcal{E})$. However, for the process-induced defect which is positively charged before electron capture, the expected lowering of the barrier potential according to the Poole-Frenkel[3,4] effect, experienced by some of the attractive centers, is not observed. This result is similar to those of Braun *et al.*[6] and Grimmeiss *et al.*[7] reported for the hole-thermal emission rate of the gold acceptor. Finally, we conclude, that for the donor process-induced as well as for the gold-acceptor defects, the surrounding potential cannot be simply considered as Coulombic.

D. Minority-carrier recombination properties of gold-acceptor and process-induced levels

It is now well admitted that the gold acceptor belongs to the class of nonradiative recombination levels. It clearly appears from Figs. 3(a) and (b) that this level, with the initial charge state of zero, may trap electrons and holes with, respectively, the capture cross section σ_{n0} and σ_{p0}. In contrast, Fig. 4 shows that the process-induced level has an attractive electron-capture cross section σ_{n+} while it exhibits a repulsive potential for the holes because of its donor charge state at the equilibrium. Nevertheless, it cannot be ruled out that this level acts as a recombination center. By using the powerful method of double pulse procedure,[45] the recombination behavior appears as a decrease of the DLTS peak height due to a fractional re-emission of electrons according to Eq. (9). Figure 10 shows the DLTS clear spectra resulting from the capture of holes at the negatively charged gold-acceptor level and at the neutral process-induced level with the capture cross section σ_{p-} and σ_p, respectively. From these measurements we can conclude that these two levels belong to the same group of nonradiative recombination centers. By varying J_{ph} or t_F, quantitative measurements of minority-capture cross sections can be performed. Figure 11 shows their evolution as a function of the temperature. The first important result is the very similar hole-capture cross section for the process-induced and gold-acceptor levels when they are initially in the neutral charge state. The capture cross sections are both temperature and electric field independent and close to the value quoted by Van Staa *et al.*[23] obtained in p-type silicon at zero electric field.

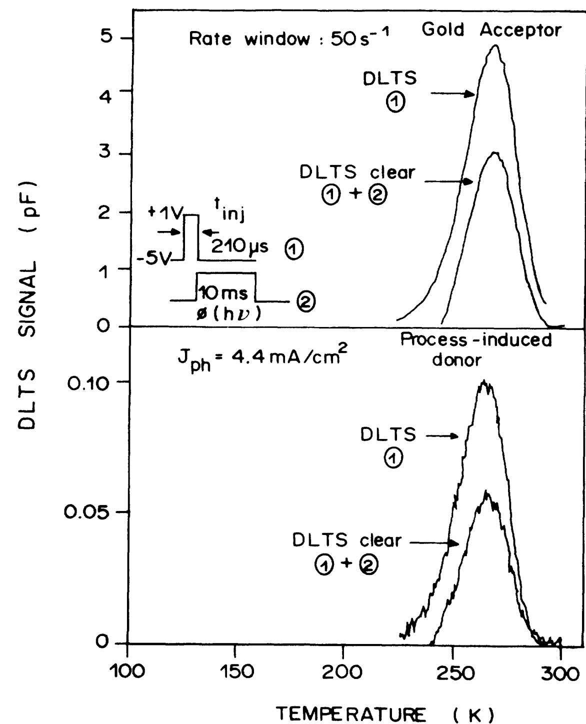

FIG. 10. DLTS and DLTS-clear spectra for the gold-acceptor and process-induced levels. The traps are filled with electrons by a 210 μs saturating electrical injection pulse followed by a 10 ms optical excitation pulse. The resulting DLTS destruction signal is due to the nonrecombined part of injected electrons.

Figure 11 also illustrates the temperature dependence of σ_{p-}. As we expect from the model of Abakumov,[12,13] dealing with the attractive centers, σ_{p-} varies as T^{-n} ($n > 2$). Our results are compared to those of Brotherton *et al.*[18] and Wu *et al.*[56] who made similar measurement of σ_{p-}; i.e., in nonzero electric fields. A comparison with the data obtained under zero-electric field, is done in Table 4 of Ref. 56. It clearly appears that the presence of an electric field during the capture process makes the temperature dependence weaker and decreases the magnitude of the capture cross section. Figure 12 shows the field dependence of σ_{p-} obtained at 251 K where the data available in the literature is also reported. A slight dependence on the field is reported by Brotherton *et al.*[18] for the gold acceptor at $\mathcal{E} < 10^4$ V/cm. However, for fields higher than 10^4

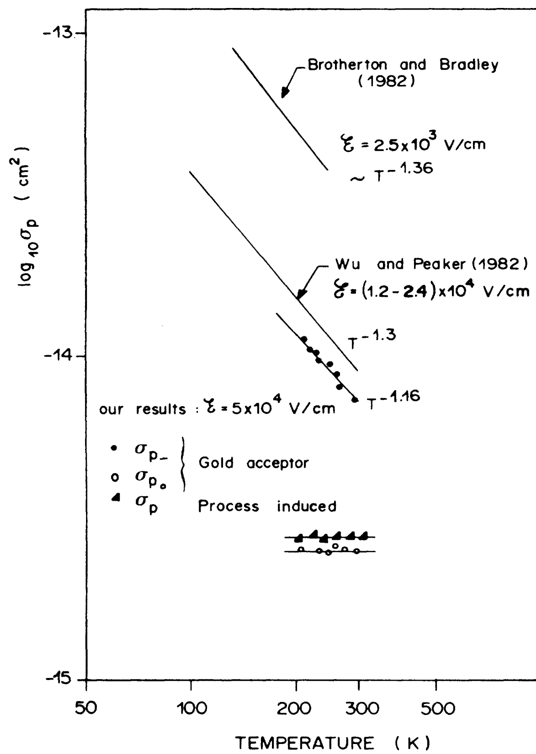

FIG. 11. Temperature dependence of the different hole-capture cross sections discussed in the text. The straight lines correspond to the best fit obtained from the literature data.

V/cm the slope increases drastically which is also the case of the process induced and the sulfur defect.[51,61] From our result, σ_{p-} is proportional to $\mathcal{E}^{-1}$ which is far from the $\mathcal{E}^{-3/2}$ prediction of Dussel *et al.*[62] and is less pronounced than the prediction of Abakumov *et al.*[63] All these authors use a Coulombic potential to build their models. In fact, the capture process by an attractive center under an external field requires to take into

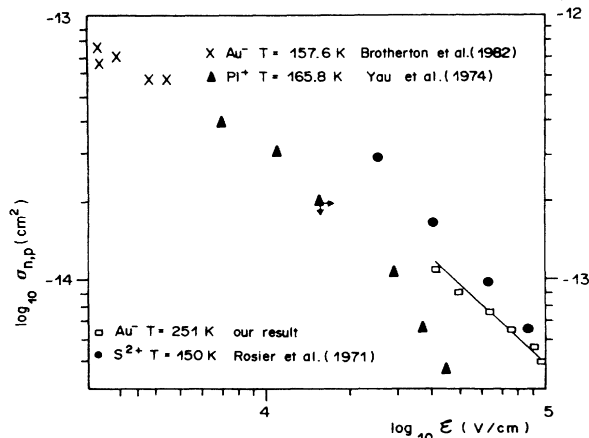

FIG. 12. Space-charge field dependence of the hole-capture cross section at the negatively charged gold-acceptor level [our result and those of Brotherton *et al.* (Ref. 18)]. Results are also reported from the literature on the electron-capture cross section of the singly ionized process induced and doubly ionized sulfur levels.

account two main parameters.

(i) The possible deformation of the bound capture orbit. We know at present that this effect takes place in a simple manner for the Coulombic potential.[3,4,63] As a consequence, the size of the capture orbit is reduced and then the capture coefficient is lowered.

(ii) The carrier heating effect[64] which is also known to decrease the capture cross section.

Theoretically, such effects responsible for the energy distribution of free carriers available for capture have been extensively studied by some authors.[62–66] However, only few experimental results are available and it is difficult to reconcile these observations with the present models. For example, according to Fig. 11, the slope of $\sigma_{p-}(T)$ seems to be well described by the cascade model of a Coulombic potential.[11,12] On the other hand, the Coulombic picture cannot explain the lack of the Poole-Frenkel effect discussed previously. The disagreement is more pronounced for the process-induced defect for which the temperature dependence of σ_n ($\propto T^{-1}$) is too low to be correlated with the Abakumov's[12] model. In this case it seems to be reasonable in a first approximation to correct the Coulombic potential by a screening function[56] proportional to $\exp(-bx)$ (b is a constant) due to the presence of a high density of free electrons in the neighborhood of the defect during the capture process ($\mathcal{E}=0$).

In addition, considering that our measurements and those of the literature have been carefully performed, we conclude that the "classical" Coulombic potential is not rigorously the appropriate model applicable to the defects reported in Fig. 12.

V. DISCUSSION

The results we presented on the gold-acceptor and process-induced levels show that, beside the parallel behavior of the thermal-emission rates pointed out by Lang,[10] we observe very strong similarities of the thermal and electrical properties of these two levels. Three major points emerge from our work.

(1) The electron thermal-emission rates and the capture cross sections of the two levels lying in the midgap behave similarly. In particular, they do not exhibit any field effect or slightly for the capture cross sections. This behavior is quite consistent with the polarization potential attributed to the neutral gold acceptor by Lax.[11] However, it is unexpected from the positively charged process-induced defect, as well as from other reported defects,[6,7] which should exhibit a Poole-Frenkel effect if they were surrounded by a Coulombic potential.

Therefore, in the light of our observations and those emerging from many other approaches in the literature,[2] we can conclude that if for isolated impurities the Coulombic pattern remains valid, the crystal formation of structural complexes may complicate the resulting potential of the defect. Consequently, the way the bound states are distributed in the potential might be a property of the chemical nature of the impurity while the ground state of the group of impurities (Ag, Au, Co, Rh, S) lying near the midgap in silicon could be determined

by the process-induced defect.[10]

(2) The gold-acceptor and the process-induced levels act as recombination-generation centers so that, in practice, it would be very convenient to use rapid thermal treatment as a procedure of limiting carrier lifetime. At this stage of our discussion, it is of interest to compare the total entropy of creation of e-h pairs via the gold-acceptor and process-induced levels with respect to the entropy associated with the direct creation of e-h pairs. Lang *et al.*[10] have discussed the first level in detail. They find that the silicon gap entropy ($\Delta S_{cv}=2.7$ K) is two times lower than the corresponding value via gold-acceptor level and propose three major explanations to this deviation.

(i) Even though it is well known that the thermal-emission rate is field independent, a small electric field may affect the emission rate so greatly as to invalidate the detailed balanced relationship used to determine the entropy factor.

(ii) The entropy factor must be corrected to the temperature dependence of the activation enthalpies $\Delta H_{n,p}(T)$ which are implicitly assumed to be constants. In other words, the level has to be considered as pinned to the conduction or the valence band.

(iii) The gold-acceptor defect is not a simple substitutional atom but a complex of Au interstitial with a vacancy. According to this model, the final state (after creation of e-h pair) could have a lower energy than the initial state (before creation of e-h pair).

For the process-induced level the same analogy holds where the total entropy of creation of an e-h pair via this level is very close to ΔS_{cv}. The ΔS_p value is deduced from the hole thermal-emission rate $e_p(T)$ obtained by measuring the reverse current. We obtain $\Delta S_p=0.9$ K and from Table I the total entropy is $\Delta S_h+\Delta S_p=2.4$ K which is very close to ΔS_{cv}. Thus assumption (i) is rejected because of the similarity of $e_n(\mathcal{E})$ for the two levels. On the other hand, due to the fact that the entropy is a direct measure of the temperature dependence of the Gibbs free energy according to Eq. (15) in Ref. 10, and because of the closer values of ΔS_n and ΔS_p found in this work for the process-induced defect, we conclude that this level has a temperature-independent position in the gap. Therefore, the conservation of energy is well obeyed during the e-h pair generation and then the ground-state energy remains constant. This is not true for the gold-acceptor level and so assumptions (ii) and (iii) seem to be valid. Further analyses on the Ag, Co, Rh, and S would be of great importance in order to better understand the apparent discrepancy discussed by Lang *et al.*[10]

(3) The formation of the process-induced defects is controlled by three parameters. The first one, not reported in Yau's experiments is the role of oxygen in the stability of the $E-0.56$ eV level. As shown in Fig. 13, at high temperatures ($\geq 1000\,^{\circ}$C), in materials containing large concentrations of oxygen ($\geq 10^{17}$ cm^{-3}), the vacancies are trapped by the oxygen atoms and the V-O centers seem to be more stable than the vacancy complex. The role of oxygen is strongly dependent on the cooling rate.[50] This parameter might explain why Sah

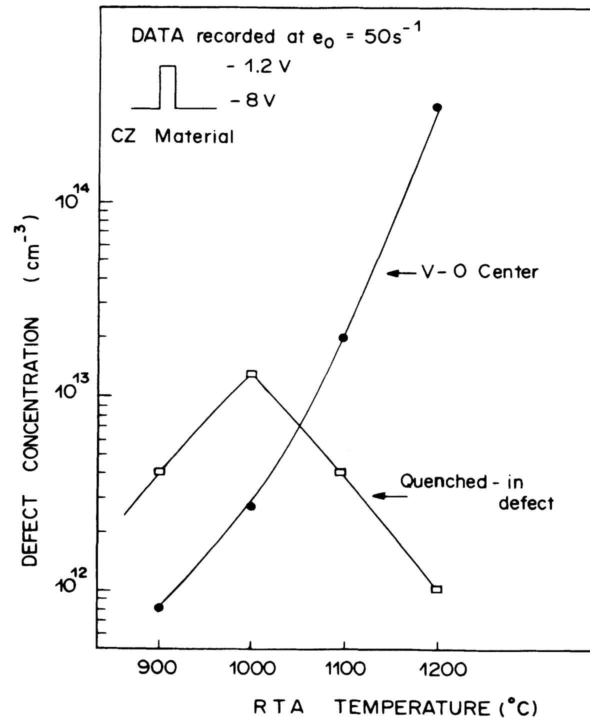

FIG. 13. Evolution of the densities of the V-O center and the process-induced defect as a function of the quenching temperature.

and Wang[67] did not observe any oxygen effect.

The second parameter concerns the possible modification of the charge state of the defects during their diffusion because of the high density of photons at short wavelengths (<1.1 μm) used for the thermal process in our RTA procedure.[50] This effect has been investigated previously using classical furnaces.[68]

Finally, the defect density is strongly dependent on surface properties. Using bright etched surfaces, we have shown that low densities of the process-induced defects are observable. Thus as pointed out by Sah and Wang[67] the donor level at $E_c-0.56$ eV is associated with the presence of highly strained surface layers from incomplete chemical etching or damaged surface. In other words, the surface acts as a source of vacancies which at high temperature diffuse rapidly into the bulk and control the final profile of the defects. This profile is strongly correlated to the distribution of gold impurity[69] and suggests that the process-induced defects control the diffusion of such impurities to the final state. This is demonstrated in Fig. 14 where we have shown the distribution of the gold acceptor after gold evaporation on two kinds of surfaces followed by a rapid thermal diffusion. The high concentration of vacancies at the surface coupled to the rapid quenching conditions seems to increase the density of gold in the electrically active position. However, the final state is not necessarily a simple substitutional site.[2,58] Thus at the end of the diffusion it is very likely to encounter numerous complexes of Au such as Au-O, Au-P, and also vacancies. More recently, Stolwijk *et al.*[70] have shown the ability of

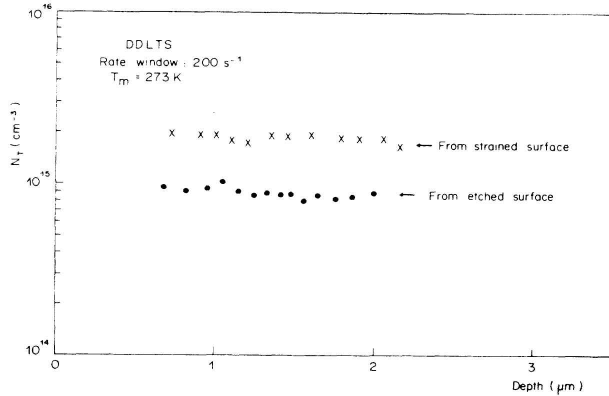

FIG. 14. Gold-acceptor defect concentration profiles as a function of the prepared surface prior to three successive cycles of RTA treatment (1000 °C for 40 s) followed by a quenching to 25 °C at 300 °C/s. The profiles are recorded after removing 25 μm in order to satisfy the uniformity of N_T and the condition $N_T < N_D$.

gold to diffuse along dislocations as extended complexes of vacancies.

VI. CONCLUSION

In this work we give a direct comparison of the electrical properties of the process-induced defect with the gold acceptor in silicon. Schottky diodes were made and the classical DLTS coupled to optical analysis were used in order to investigate the whole band gap. The major interest for the optical procedure is that the duration of the capture transient taking place in the high region can be easily controlled by the photocurrent. Also long transients in the range of hundreds of milliseconds can be readily obtained. Moreover, the field-dependence measurement of the capture cross section may be a useful source of information on the structure and long-range potential of the centers. Unfortunately, significant nonlinear behaviors might complicate the data treatment. It is, therefore, necessary to model the spatial-dependent carrier capture rate numerically in order to match the theory and the experiment quite well. We find the concentration of the gold acceptor is about five times higher than that of the gold donor; however, we observe a complete hydrogen passivation of both levels. We also find that the hole-capture cross section of the gold donor in n-type silicon is nearly an order of magnitude larger than in p-type silicon. It appears to us that the gold donor does not behave similarly in the two types of material.

The second part of this work indicates that the gold acceptor and the process-induced donor levels have basically similar electron thermal relaxations. This parameter is field independent up to 10^5 V/cm as expected for the neutral gold acceptor, but not for the donor process-induced defect. This suggests that the Poole-Frenkel model should not be systematically used, but that other mechanisms have to be taken into account in order to approach the physical reality.

We have shown that the total entropy associated with the direct creation of e-h pairs via the process-induced level is close to the entropy of the silicon gap. This result is consistent with the temperature-independent energy position in the gap. On the other hand, we suggest that the ground state of the $E_c-(0.55\pm0.01)$ eV level is probably a characteristic of the process-induced defect and is insensitive to any external force. It is also insensitive to applied electric fields or a more localized field of an impurity such as gold. Finally, our observations are consistent with the model suggested by Lang *et al.*[10] where the process-induced defect could be the basic defect of the gold acceptor and probably of the family of four other impurities (Ag, Co, Rh, S). These impurities are "driven" by the process-induced defect which constitutes a large complex of vacancies. The final state is still characterized by the electron thermal-emission rate of the process-induced level while the defect wave function, the magnitude of ΔS_n, σ_n, and the final charge state are functions of the chemical nature of the impurity. Further detail from the studies on the above-mentioned impurities would be of great importance in order to have more physical information.

ACKNOWLEDGMENTS

This work was supported by the Agence Française pour la Maitrise de l'Energie (AFME). A Mesli wishes to express his gratitude to Professor C. T. Sah for his stimulating and informative remarks. The authors would also like to thank Dr. M. Samimi and Dr. J. P. Ponpon for their useful comments on this work.

APPENDIX

The method of measuring the electric field dependence of the thermal-emission rate used by Sah *et al.*[30] is based on the variation of the height of the electric pulse applied to the device. The low level of the pulse or reverse biase (V_r) is kept constant while the high level (or injection level V_I) is varied. Thus the depleted layer W_r (for a given V_r) is divided into two regions. The deeper part $W_I < x < W_r$ where the trap is filled, and the superficial part $0 < x < W_I$ where the trap remains empty. Following the procedure of Sah and Fu,[28] W_r is constant while W_I goes from zero to a value closer to W_r. In fact, we must take into account the transition region (λ_r) where the trap remains filled at any time (see Fig. 1 in the text). Note that λ_r is independent of the voltage V_I. The working equation derived from Poisson's equation is given by

$$V_r = -\frac{q}{\epsilon_r}\int_0^{W_r(t)-\beta\lambda_r}[N_D(x)-n_T(x,t)]x\,dx \ . \quad \text{(A1)}$$

Here $\beta=0$ or $\beta=1$ according to whether or not we neglect the transition region. For an acceptorlike defect. Eq. (A1) can be written as follows:

$$V_r = -\frac{q}{\epsilon_r}\left[\int_0^{W_I-\beta\lambda_r} N_D(x)x\,dx + \int_{W_I-\beta\lambda_r}^{W_r(t)-\beta\lambda_r} [N_D(x)-n_T(x,t)]x\,dx\right] . \quad \text{(A2)}$$

The procedure of Sah *et al.*[28] consists of differentiating Eq. (A2) with respect to $V_I(\delta/\delta V_I)$ using the well-known mathematical relation

$$\frac{\delta}{\delta\alpha}\int_{a(\alpha)}^{b(\alpha)} f(x)dx = f(b)\frac{\delta b}{\delta\alpha} - f(a)\frac{\delta a}{\delta\alpha} .$$

By transforming $W_r(t)$ and W_I to the measured high-frequency capacitance according to

$$W_r(t) = \epsilon_r S C_r(t)^{-1}, \quad W_I = \epsilon_r S C_I^{-1} ,$$

and using Eq. (A2) after its differentiation, we get

$$N_D(W_I)\left[\frac{\delta C_r^{-2}}{\delta C_I^{-1}} - \frac{2\beta\lambda_r}{\epsilon_r S}\frac{\delta C_r^{-1}}{\delta C_I^{-1}}\right] = n_T(W_I,t)\left[\frac{\delta C_r^{-2}}{\delta C_I^{-1}} - \frac{2}{C_I} - \frac{2\beta\lambda_r}{\epsilon_r S}\left[\frac{\delta C_r^{-1}}{\delta C_I^{-1}} - 1\right]\right] , \quad \text{(A3)}$$

where N_D and N_T are considered as uniform, and

$$n_T(W_I,t) = N_T(W_I)\exp[-e_n(W_I)t] .$$

To obtain the field dependence of the time constant (or thermal-emission rate), (A3) can be differentiated with respect to time and the results evaluated at a predetermined time t_0 according to

$$e_n(W_I) = \frac{N_D - N_T}{N_T}\,\frac{\left[\frac{\delta}{\delta t}\frac{\delta C_r^{-2}}{\delta C_I^{-1}}\right]_{t_0} - \frac{2\beta\lambda_r}{\epsilon_r S}\left[\frac{\delta}{\delta t}\frac{\delta C_r^{-1}}{\delta C_I^{-1}}\right]_{t_0}}{\left[\frac{2}{C_I} - \frac{\delta C_r^{-2}}{\delta C_I^{-1}}\right]_{t_0} + \frac{2\beta\lambda_r}{\epsilon_r S}\left[\frac{\delta C_r^{-1}}{\delta C_I^{-1}} - 1\right]_{t_0}} . \quad \text{(A4)}$$

A similar relation is obtained for a donorlike defect. The relation (10) of Ref. 28 corresponds to Eq. (A4) where $\beta=0$ and $N_T \ll N_D$. When the pulse height decreases, the effective volume of trapped carriers also decreases and becomes comparable to the transition region. Thus in Eq. (A2) the term allowing λ_r cannot be neglected.

[1]U. Llindefelt and A. Zunger, Phys. Rev. B **30**, 1102 (1984).
[2]A. Fazzio, M. J. Caldas, and A. Zunger, Phys. Rev. B **32**, 934 (1985).
[3]U. Frenkel, Tech. Phys. USSR **5**, 685 (1938); Phys. Rev. **54**, 647 (1938).
[4]J. L. Hartkee, J. Appl. Phys. **39**, 4871 (1968).
[5]A. F. Tasch, Jr., and C. T. Sah, Phys. Rev. B **1**, 800 (1970).
[6]S. Braun and H. G. Grimmeiss, Solid State Commun. **11**, 1457 (1972).
[7]H. G. Grimmeiss, Ann. Rev. Mater. Sci. **7**, 341 (1977).
[8]L. C. Kimerling and J. L. Benton, Appl. Phys. Lett. **39**, 410 (1981).
[9]R. D. Harris, J. L. Newton, and G. D. Watkins, Phys. Rev. Lett. **48**, 1271 (1982).
[10]D. V. Lang, H. G. Grimmeiss, E. Heijer, and M. Jaros, Phys. Rev. B **22**, 3917 (1980).
[11]M. Lax, Phys. Rev. **119**, 1502 (1960).
[12]V. N. Abakumov and I. N. Yassievich, Zh. Eksp. Teor. Fiz. **71**, 657 (1976) [Sov. Phys.—JETP **44**, 345 (1976)].
[13]V. N. Abakumov, V. I. Perel, and I. N. Yassievich, Fiz. Tekh. Poluprovodn **12**, 3 (1978)] [Sov. Phys. Semicond. **12**, 1 (1978)].
[14]H. Gummel and M. Lax, Phys. Rev. **97**, 1469 (1957).
[15]V. A. Kovarskii, Fiz. Tverd, Tela. (Leningrad) **4**, 1636 (1962) [Sov. Phys. Solid State **4**, 1200 (1962].
[16]E. P. Sinyavskii and V. A. Kovazskii, Fiz. Tverd. Tela (Leningrad) **9**, 1464 (1966) [Sov. Phys. Solid State **9**, 1142 (1967)].
[17]C. H. Henry and D. V. Lang, Phys. Rev. B **19**, 989 (1977).
[18]S. D. Brotherton and P. Bradley, J. Appl. Phys. **53**, 1543 (1982).
[19]Luke Su Lu and C. T. Sah, J. Appl. Phys. **59**, 173 (1986).
[20]S. D. Brotherton, P. Bradley, and A. Gill, J. Appl. Phys. **55**, 952 (1984).
[21]L. A. Ledebo and Z. G. Wang, Appl. Phys. Lett. **42**, 680 (1983).
[22]J. Utizig and W. Schroter, Appl. Phys. Lett. **45**, 761 (1984).
[23]P. Van Staa and R. Kassing, Solid State Commun. **50**, 1051 (1984).
[24]R. M. Fenestra and S. T. Pantelides, Phys. Rev. B **31**, 4083 (1984).
[25]S. J. Pearton and A. J. Tavendale, Phys. Rev. B **26**, 7105 (1982); Appl. Phys. Lett. **41**, 1145 (1982).
[26]S. J. Pearton, W. L. Hansen, E. E. Haller, and J. M. Kahn, J. Appl. Phys. **55**, 1221 (1984).
[27]A. C. Wang and C. T. Sah, J. Appl. Phys. **57**, 4645 (1985).
[28]C. T. Sah and H. S. Fu, Phys. Status. Solidi A **14**, 59 (1972).
[29]C. T. Sah, L. Forbes, L. L. Rosier, and A. F. Tasch, Jr., Solid State Electron. **13**, 759 (1970).
[30]D. V. Lang, J. Appl. Phys. **45**, 3023 (1974).
[31]L. C. Kimerling, J. Appl. Phys. **45**, 1838 (1974).
[32]E. Meijer, L. A. Ledebo, and Z. G. Wang, Solid State Commun. **46**, 255 (1983).
[33]S. D. Brotherton, P. Bradley, and J. Bicknell, J. Appl. Phys. **50**, 3396 (1979).
[34]H. G. Grimmeis, L. A. Ledebo, and E. Meijer. Appl. Phys. Lett. **36**, 307 (1980).

[35]A. Zylbersztejn. Appl. Phys. Lett. **33**, 200 (1978).

[36]J. A. Borsuk and R. M. Swanson, J. Appl. Phys. **52**, 6704 (1981).

[37]D. V. Lang, in *Thermally Stimulated Relaxation Process in Solids,* edited by P. Braunlich (Springer-Verlag, New York, 1979), p. 93.

[38]B. Hamilton, A. R. Peaker and D. R. Wight, J. Appl. Phys. **50**, 6373 (1979); F. Brunwin, B. Hamilton, P. Jordan, and A. R. Peaker, Electron. Lett. **15**, 348 (1979); A. R. Peaker, F. Brunwin, P. Jordan, and B. Hamilton, *ibid.* **15**, 663 (1979).

[39]H. F. Wolf, in *Silicon Semiconductor Data* (Pergamon, New York, 1967), p. 76.

[40]C. Jacoboni, C. Canali, G. Ottaviani, and A. A. Quaranta Solid-State Electron. **20**, 77 (1977).

[41]E. H. Rhoderick, in *Metal-Semiconductor Contacts* (Clarendon, Oxford, 1978), p. 142.

[42]H. C. Card. Solid State Electron. **30**, 971 (1977).

[43]L. C. Olsen, Solid State Electron. **30**, 741 (1977).

[44]G. Vincent, Appl. Phys. **23**, 215 (1980); Ph.D. Thesis, Lyon University, 1978 (unpublished).

[45]D. V. Lang, J. Appl. Phys. **45**, 3014 (1974).

[46]J. E. Stannard, H. M. Day, H. L. Bark, and S. H. Lee, Solid State. Electron. **24**, 1009 (1981).

[47]C. M. Ransom, T. I. Chapell, J. L. Freeouf, and P. D. Kirchner, in *Proceedings of the Materials Research Society Conference on Materials Characterization, Palo Alto, 1986,* edited by N. W. Cheung (Publisher, City, 19xx). (North Holland, New York–Oxford, 1986).

[48]S. D. Brotherton and J. E. Lowther, Phys. Rev. Lett. **44**, 606 (1979).

[49]E. V. Astrova, V. B. Voronkov, A. A. Lebedov, and B. M. Urunbaev, Fiz. Tekh. Poluprovodn. **29**, 1709 (1985) [Sov. Phys. Semicond. **19**, 1051 (1985)].

[50]A. Mesli (unpublished).

[51]L. D. Yau and C. T. Sah, Solid State Electron. **17**, 193 (1974).

[52]S. T. Brierley, J. Appl. Phys. **59**, 168 (1986).

[53]L. Stolt and K. Bohlin. Solid State. Electron. **28**, 1215 (1985).

[54]R. Sh. Malkovich and V. A. Poloeva, Fiz. Tverd. Tela (Leningrad) **18**, 2606 (1976) [Sov. Phys. Solid State **18**, 1521 (1976)].

[55]L. V. C. Assali and J. R. Leite, Phys. Rev. Lett. **26**, 980 (1985).

[56]R. H. Wu and A. R. Peaker, Solid State Electron. **25**, 643 (1982).

[57]R. Kassing, L. Cohansz, P. Van Staa, W. Mackert, and H. J. Hoffman, Appl. Phys. A **34**, 41 (1980).

[58]J. A. Van Vechten and C. D. Thurmond, Phys. Rev. B **14**, 3539 (1976).

[59]S. M. Sze, in *Physics of Semiconductors* (Wiley, New York, 1969).

[60]O. Engstrom and H. G. Grimmeiss, J. Appl. Phys. **46**, 831 (1975).

[61]L. L. Rosier and C. T. Sah, Solid State Electron. **14**, 41 (1971).

[62]G. A. Dussel and R. h. Bube, J. Appl. Phys. **37**, 2797 (1966); G. A. Dussel and K. W. Boer, Phys. Status Solidi **39**, 375 (1970).

[63]V. N. Abakumov, L. N. Kresshchuk, and I. N. Yassievich, Fiz. Tekl. Poluprovodn. **12**, 152 (1978) [Sov. Phys. Semicond. **12**, 152 (1977)].

[64]A. I. Veinger, V. G. Ivanov, L. G. Paritskii and S. M. Pyvkin, Fiz. Tekh. Poluprovodn. **12**, 1480 (1968) [Sov. Phys. Semicond. **2**, 1236 (1968)]; R. Passler, Solid State Electron. **27**, 155 (1984).

[65]E. E. Godik, Yu. A. Kuritsyn, and V. P. Sinis, Fiz. Tekh. Poluprovodn. **12**, 351 (1978) [Sov. Phys. Semicond. **12**, 203 (1978)].

[66]B. Oejnikova, Phys. Status Solidi B **108**, 79 (1981); V. Ya. Prinz and S. N. Rechtunov, *ibid.* **118**, 159 (1983).

[67]C. T. Sah and C. T. Wang, J. Appl. Phys. **46**, 1767 (1975).

[68]L. C. Kimerling, H. M. De Angelis, and C. P. Carnes, Phys. Rev. B **3**, 427 (1971); L. C. Kimerling and C. P. Carnes, J. Appl. Phys. **42**, 3548 (1971).

[69]F. A. Huntley and A. F. W. Willonghby, Solid State Electron. **13**, 1231 (1970); J. Martin, E. Haas, and K. Raithel, *ibid.* **9**, 83 (1966).

[70]N. A. Stolwijk, J. Holzl, W. Franck, E. R. Weber, and H. Nehrer, Appl. Phys. A **39**, 37 (1986).